Green Chemistry

PAPER

View Article Online
View Journal | View Issue

Check for updates

Cite this: *Green Chem.*, 2025, **27**, 670

Waste-based value-added feedstocks from tire pyrolysis oil distillation: defossilization of the petrochemical industry†

Juan Daniel Martínez, *[a] Alberto Sanchís, [a] Alberto Veses, [a] Andreas Kapf,[b] José Manuel López, [a] María Soledad Callén, [a] Tomás García [a] and Ramón Murillo [a]

The recovery of waste-based feedstocks is an important step in the defossilization of the petrochemical industry and thus in the circular economy for petroleum-based products that have reached the end of their useful life such as end-of-life tires (ELT). This work is part of the European BLACKCYCLE project, and focuses on the distillation performance of tire pyrolysis oil (TPO) obtained from an industrial scale plant, ranked at the ninth technology readiness level (TRL-9). The influence of different reboiler temperatures and reflux ratios on the yields and characteristics of the resulting streams was investigated using a pilot scale packed distillation column under industrially relevant conditions, classified within the fifth technology readiness level (TRL-5). The distillation process was shown to be capable of continuously producing a light fraction (LF) with a very high concentration of benzene, toluene, ethylbenzene and xylenes (BTEX) suitable for high value chemicals. Similarly, a heavy fraction (HF) with a high C/H ratio, high flash point and high presence of polycyclic aromatic hydrocarbons (PAH) is obtained, making it an attractive alternative to carbon black oil. These results are quite outstanding to accomplish the recovery of waste-based value-added feedstocks in such a way that the carbon embedded in the ELT is retained in the petrochemical industry. This work is committed to the development of green, affordable and practical recycling processes to fill the gap in the production of sustainable chemical commodities, while paving the way to address one of the industry's greatest challenges: the defossilization of the petrochemical industry.

Received 15th October 2024,
Accepted 28th November 2024

DOI: 10.1039/d4gc05185h

rsc.li/greenchem

Open Access Article. Published on 03 December 2024. Downloaded on 2/20/2026 11:20:57 AM.
This article is licensed under a Creative Commons Attribution 3.0 Unported Licence.

1. Introduction

The recycling of post-consumer products such as end-of-life tires (ELT) has become a major challenge worldwide, not only because they are designed to be robust and extremely durable, but also because they are very resistant to biological and chemical treatments (difficult to degrade under typical environmental conditions). In addition, they are continuously generated due to the increasing tire demand. The total amount of tires worldwide was estimated at 30.9 Mt in 2019,[1] and the annual growth rate is expected to be 3–4% in the coming years.[2] Although most of the ELT generated in developed countries are processed by material and energy recovery processes, significant amounts accumulate in landfills or open fields in developing countries.[3] Material recovery includes the production of chips, granules and powders for various civil engineering applications, and even as a preliminary step for energy recovery, which ultimately uses the ELT as a fuel. However, current circular economy regulations aim to recover secondary raw materials that allow carbon to be retained rather than significantly degraded. Therefore, the use of ELT as fuel in combustion systems results in a poor return on value not only because the carbon is degraded to CO_2, but also because only a very small amount of energy is recovered (30–35 MJ kg^{-1}) compared to the high energy input required to produce a tire (200 MJ kg^{-1}).[1]

Situated below "reuse" in the waste hierarchy, recycling is expected to contribute significantly to the defossilization and circular economy of most of society's petroleum-based products. In particular, the recycling of ELT should retain the embedded tire carbon to enable a carbon-based petrochemical industry to become circular. This approach enables the transition from a linear to a circular carbon economy while addressing waste management. In addition, the recovery of carbochemicals is an excellent example of how the petrochemical industry can implement defossilization processes by displacing as much fossil crude oil as possible. Petrochemicals, indispensable to modern society, involve diverse carbon-inten-

[a]*Instituto de Carboquímica (ICB-CSIC), Miguel Luesma Castán 4, 50018 Zaragoza, Spain. E-mail: jdmartinez@icb.csic.es*
[b]*Pyrum Innovations AG, Dieselstraße 8, D-66763 Dillingen, Germany*
† Electronic supplementary information (ESI) available. See DOI: https://doi.org/10.1039/d4gc05185h

This journal is © The Royal Society of Chemistry 2025

Open Access Article. Published on 03 December 2024. Downloaded on 2/20/2026 11:20:57 AM. This article is licensed under a Creative Commons Attribution 3.0 Unported Licence.

sive activities that are accompanied by negative externalities due to the high resulting carbon footprint. This is due to the greenhouse gas emissions associated not only with fossil fuel-fired heating systems, but also with the fossil feedstock itself from which the petrochemical commodity is derived. Efforts to reduce the former greenhouse gases are referred to as decarbonization, while efforts to replace carbon in chemical products through the use of recovered feedstocks or renewable sources are referred to as defossilization.[4] The petrochemical industry is projected to continue to grow and recognizes the limited capacity of the earth to provide conventional fossil carbon feedstocks to meet the challenges ahead.[5] Therefore, alternative carbon sources from renewable sources such as biomass and end-of-life products are expected to play an important role, as well as CO_2 (from CCS/CCU: carbon capture sequestration and carbon capture utilization) when conversion technologies are fully developed and economically competitive[5] (Fig. 1).

Mechanical and chemical recycling is a collection of different technologies that transform polymer waste such as ELT into various secondary raw materials including base chemicals and monomers. Both approaches are complementary, and are expected to help in bridging the gap between waste management and the petrochemical industry.[5–8] Pyrolysis is a thermochemical process that falls under the general definition of chemical recycling because it changes the chemical structure of the waste.[9] Pyrolysis is currently experiencing an outstanding surge and is likely the leading technology for thermochemical recycling of complex waste such ELT due to its flexibility, robustness, and more recently, favorable economics. Defined as the thermochemical breakdown of macromolecules by energization with heat and usually in the absence of oxygen,[10] pyrolysis is capable to digging out the embedded value of the ELT.[11] During this process, the rubber compounds (natural rubber, butyl rubber and styrene–butadiene rubber) are separated from the non-volatile components (carbon blacks, SiO_2, ZnO, *etc.*).[12,13] Thus, the pyrolysis of ELT produces tire pyrolysis gas (TPG) and tire pyrolysis oil (TPO) associated with the volatile compounds, and raw recovered carbon black (RRCB) related to the carbon blacks used in tire manufacturing. TPG has a remarkable calorific value with important concentrations of H_2, and CH_4, among others, and is capable of providing the energy required by pyrolysis. TPO is an interesting mixture of liquid hydrocarbon compounds, and typically contains single aromatic compounds such as benzene, toluene, ethylbenzene, and xylenes (BTEXs), as well as heavier hydrocarbon complexes.[14,15] RRCB can be improved by milling to enhance reinforcing properties. In this case, and once wires and fabrics have been removed, this fraction should be referred to recovered carbon black (rCB) in accordance with ASTM standard D8178.[16] Pyrolysis offers a valuable way to turn the ELT to secondary raw materials for making products, and acts as an environmentally sound alternative to others pathways of the waste hierarchy.[17]

The highest yields from the pyrolysis of ELT are RRCB (35–45 wt%) and TPO (30–50 wt%).[12,13] The former continues to pursue a market niche from a circular economy perspective as a substitute for virgin carbon black, with active support from ASTM, as evidenced by recently published standards.[16,18,19] The latter also offers interesting possibilities for use as a substitute for fossil resources in the petrochemical industry, particularly for the extraction of high value chemicals such as BTEX, as well as heavy hydrocarbon feedstocks for carbon black production. The BTEX is one of the top 15 petrochemical commodities[20] and has been produced using fossil fuels.[21] These monoaromatics are key platform chemicals for the production of multiple derivatives[22] or in other words, drive the global consumption of various chemicals, plastics, synthetic fibers and rubber, among others.[23] On the other hand, carbon black is also an interesting global commodity, listed as one of the top 50 industrial chemicals with a wide range of applications, the tire industry being the largest application.[24] Carbon black is typically produced from high molecular weight hydrocarbon-based feedstocks that are rich in aromatics such as coal tar and from the bottoms of steam crackers and fluid catalytic crackers.[25] Therefore, the recovery of BTEX and raw materials for carbon black production from TPO is considered a very attractive option for defossilization in the petrochemical industry, especially considering the enormous potential of many operating refineries to become "waste refineries" as suggested elsewhere.[26]

Among other benefits, the recovery of these feedstocks from end-of-life products minimizes dependence on non-renewables sources and provides a significant boost to the circular economy. Most chemicals and products are based on finite fossil resources and are therefore highly vulnerable to volatile oil prices, in addition to having high CO_2 emissions. The petrochemical subsector is difficult to defossilize not only because of the high heat input required to drive the refinery operations, but also because the raw materials used to produce these commodities are derived from fossil resources, as discussed above. The industrial sector (8.7 Gt CO_2 per y) is the second-largest CO_2 emitter after the electricity sector (12.3 Gt CO_2 per y), and includes the petrochemical, iron, steel, and cement subsectors, among others.[27,28] Roughly speaking, the

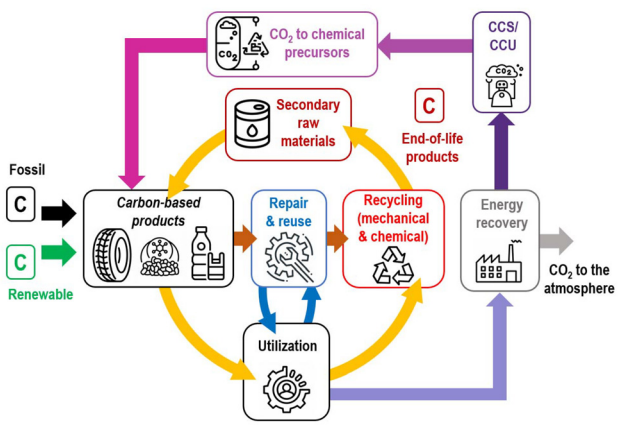

Fig. 1 Schematic representation of the carbon circular economy.

Open Access Article. Published on 03 December 2024. Downloaded on 2/20/2026 11:20:57 AM.
This article is licensed under a Creative Commons Attribution 3.0 Unported Licence.

primary energy consumption of these subsectors in 2019 accounted for 1005, 800 and 250 Mtoe per y, respectively, making the petrochemical subsector the largest energy consumer, ahead of the steel and cement subsectors.[27,28]

This work was carried out as part of the BLACKCYCLE project and demonstrates, under relevant industrial conditions, the recovery of BTEX and raw materials for carbon black production by distillation using a packed column operating in continuous mode. The distillation plant has been designed and erected specifically to operate with TPO, and is at the fifth technological readiness level (TRL-5).[11,29] An extensive experimental campaign was conducted to evaluate the effect of reboiler temperature and reflux ratio on the resulting distillation yields, namely the light fraction (LF), which contains the BTEX compounds, and the heavy fraction (HF), which is considered as a feedstock for carbon black production. The TPO used in the distillation unit was obtained from an industrial-scale pyrolysis plant based on the moving bed reactor, which aligns with the ninth technological readiness level (TRL-9).

This work is committed to the development of green, affordable and practical recycling processes to fill the gap in the production of sustainable chemical commodities. In addition, the pyrolysis process of ELT and the refinement/separation of value-added chemicals at a high level of technological maturity exemplifies one of the major challenges for the development of industrial green chemistry around end-of-life products. In this way, this work represents an opportunity to address these challenges by demonstrating not only that the industrial-scale pyrolysis process is real, but also that the production of important, marketable, high-value chemicals that can replace petroleum-based feedstocks is well on its way to industrial deployment. Moreover, as stated by García-García *et al.*,[30] the pyrolysis of end-of-life products is fully consistent with the engineering principles of green chemistry[31] in particular atom economy (principle 2) and design for energy efficiency (principle 6). With respect to the principle 2, pyrolysis allows virtually all of the atoms present in the ELT to be reused, in this case as chemical precursors, thus avoiding the generation of waste. This work focuses on TPO using an industrially relevant conditions distillation column to recover BTEX and an alternative feedstock to carbon black oil, demonstrating how crude oil could be displaced in the petrochemical industry. Regarding principle 6, pyrolysis requires energy to drive the endothermic reactions, and this energy could be obtained by using the TPG as a fuel in order to produce either hot flue gases or electricity after the use of engines/turbines. It is also worth noting that pyrolysis is closely related to the *E*-factor,[32] which in turn is closely related to the principles of green chemistry, as this process reduces the amount of final waste generated. The results presented here, are expected to positively impact the goals of the EU Green Deal and some of the UN Sustainable Development Goals (7, 11, 12 and 13), by pursuing the production of waste-based chemical commodities through a circular economy strategy that integrates a pyrolysis technology at TRL-9 and a distillation unit at TRL-5.

2. Materials and methods

2.1. Pyrolysis

The TPO used in this work was produced by Pyrum Innovations AG, which uses a patented moving bed reactor technology to perform the pyrolysis of ELT.[33,34] The plant is located in Dillingen/Saar (Germany) and is capable of processing about 5000 t per y of shredded ELT. Following its development and commissioning in 2015, the plant is currently operating continuously twenty-four hours a day, seven days a week; and is therefore aligned with the ninth technological readiness level (TRL-9). A general diagram of the whole plant is shown in Fig. 2. As it is observed, the plant consists of different systems such as feeding, pyrolysis reactor, condensation, and RRCB collection and milling. The feeding system includes shredding and separation units for both wire and fabric, and delivers rubber granules (<8 mm). Both streams are separated from the ELT by magnetic and pneumatic systems, respectively, providing suitable raw materials for other processes.

The pyrolysis reactor system consists of a moving bed reactor that is electrically heated to temperatures between 500 and 750 °C. Under these conditions, Pyrum's process yields approximately 35% TPO, 45% RRCB and 20% TPG. The rubber granules are pyrolyzed from the top to the bottom by weight of the material and the residence time is determined by the dosing device installed on the reactor (at least one hour). The reactor itself is designed as a vertical, cylindrical gas-tight apparatus. The condensation unit receives the vapors generated during pyrolysis and produces both TPO and TPG. The latter is sent to a combined heat and power (CHP) unit after being filtered and purified. The electricity generated by the CHP provides the energy needed to power both the pyrolysis reactor and the RRCB mill. The RRCB is continuously extracted from the bottom part of the reactor *via* sluice systems, and then fed to the milling and pelletizing systems.

2.2. Distillation

The pilot scale distillation plant consists of a packed column and is capable of processing up to 20 kg h^{-1} of TPO, placing the plant at the fifth technological readiness level (TRL-5). Technical details are provided in other works that also demonstrate its functionality and versatility in distilling various TPOs derived from different pyrolysis technologies.[11,29] The distillation column considers eight theoretical minimum equilibrium stages, resulting in a total packing height of 3.5 m. The column has an inside diameter of 11 cm and uses randomly arranged 1″ stainless steel pall rings as packing, with openings made by folding strips of the surface into the ring (bulk density of 481 kg m^{-3} and surface area of 210 m^2 m^{-3}).

As shown in Fig. 3, the TPO is stored in two interconnected vessels (V1 and V2) and pumped to the column using a calibrated peristaltic pump (TPO pump). A guided wave radar level meter (Levelflex FMP50) connected to V2 continuously monitors the TPO level (LT2). Although in this work the TPO is fed at the center of the column, it is also possible to feed it from two other points located at the bottom (stripping section) and top of

 This journal is © The Royal Society of Chemistry 2025

Open Access Article. Published on 03 December 2024. Downloaded on 2/20/2026 11:20:57 AM.
This article is licensed under a Creative Commons Attribution 3.0 Unported Licence.

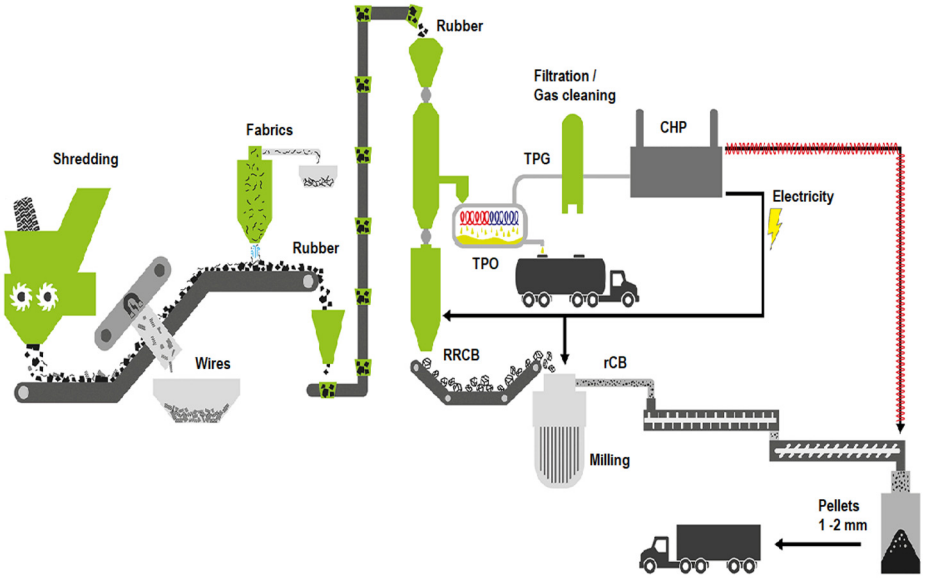

Fig. 2 General overview of the Pyrum's process for pyrolysis of ELT.

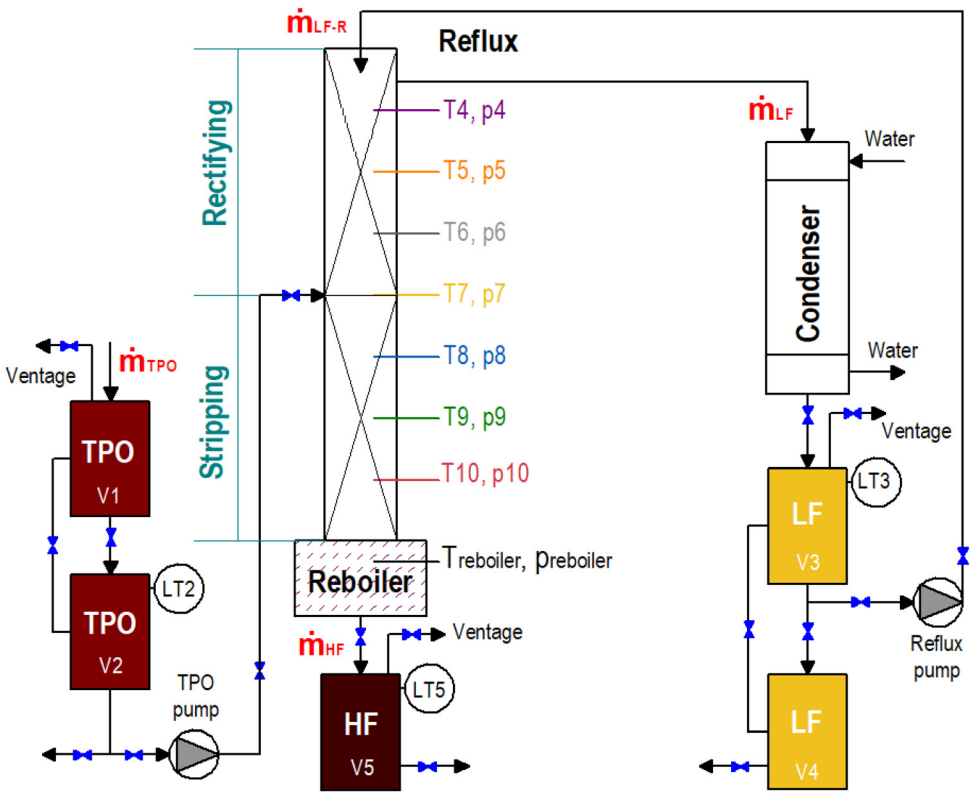

Fig. 3 General scheme of the packed distillation column for TPO.

the column (rectifying section). Each feed line is equipped with pneumatic valves that are connected to the control and acquisition system. The column is equipped with eight thermocouples (T_i) and pressure transducers (p_i) that are located along the length of the distillation column, including those of the reboiler. These signals are useful for monitoring the progress of the distillation process, *i.e.* transient and steady state, as well as for the identification of possible malfunctions.

The reboiler at the bottom of the column provides the energy for the distillation of the TPO. The reboiler consists of a

Open Access Article. Published on 03 December 2024. Downloaded on 2/20/2026 11:20:57 AM. This article is licensed under a Creative Commons Attribution 3.0 Unported Licence.

5 kW electrical resistance array immersed in the TPO. As a result, the generated vapors travel upward across the column in constant contact with the downward TPO stream. In the condenser, the low-molecular-weight vapors leaving the distillation column are recovered as liquids and are referred to as the LF. The condenser uses tap water and consists of a shell-and-tube counterflow heat exchanger. Two containers (V3 and V4) connected to each other store the LF leaving the condenser. V3 is connected to a guided wave radar level transmitter (Levelflex FMP50, LT3) and is used as a reservoir for pumping the LF to the distillation column to evaluate the reflux influence during the distillation process. V4 is used for storage and sampling. A supply line connects V3 and V4 to a second peristaltic pump (reflux pump) and the top of the column. Finally, just below the reboiler, the higher molecular weight compounds go down the distillation column. This stream is the resultant HF, which is collected in the V5 container also equipped with a guided wave radar level meter (Levelflex FMP50, LT5).

2.3. Experimental planning

This work shows the influence of the reboiler temperature (190, 210, 230, 250 and 270 °C) and reflux ratio (up to 1.5) on both LF and HF yields and composition, and the experimental campaign performed is shown in Table S1.† Based on previous distillation experiments, this temperature range was selected to recover BTEX compounds in the LF.[11,29] The reflux ratio in a packed distillation column is typically in the range of 1 to 3,[35,36] and is defined as the ratio of the liquid mass flow returned to the column to the liquid mass flow removed as product. In other words, it is the ratio between the LF returned to the distillation column ($\dot{m}_{\text{LF-R}}$) and the LF collected in T3 ($\dot{m}_{\text{LF}}$). In all cases, the TPO feed rate was 20 kg h^{-1}. There was no pre-heating of either the TPO or the reflux before it was fed to the distillation column. Temperature and pressure signals were recorded and plotted instantaneously during all tests, while LF and HF yields were determined by weighing at the end of the experiment. Each run at the distillation pilot plant takes one day and includes TPO loading, column heating, distillation, shutdown and cooling, and LF and HF discharge.

2.4. Characterization

The boiling range distribution of TPO was measured by gas chromatography (GC) using the method described in the ASTM D2887 standard, and the PerkinElmer Clarus 590. The TPO and the resulting HF were characterized in terms of elemental analysis (Thermo Flash 1112, UNE-EN 15407), heating value (Parr 6400, UNE-EN 15400), and flash point (Grabner Instruments, ASTM D6460). These analytical methods were difficult to apply to the LF samples due to the high volatility of the samples and therefore the results were not repeatable. The TPO and the HF samples were also analyzed by GC coupled to a quadrupole mass spectrometer (MS) (PerkinElmer Clarus 690 – PerkinElmer Clarus SQ 8). The system was equipped with a capillary column, Elite-5 ms (5% diphenyl-95% dimethylpolysiloxane; 60 m × 0.25 mm ID, 0.250 μm df). The identified individual compounds were 99 which were grouped into a total of six families (BTEX, substituted benzenes, indanes and indenes, heterocyclic compounds, and polynuclear aromatic hydrocarbons (PAH)) based on the percentage of relative area. All injections were performed in duplicate. In addition, all samples including the LF were analyzed by gas chromatography (PerkinElmer Clarus 590 GC) to determine the concentration of benzene, toluene, xylenes (*o*-xylene, *m*-xylene, *p*-xylene), ethylbenzene (BTEX) and limonene using a wide-range FID detector and a 60 m DB-5 ms capillary column (0.25 mm ID and 0.25 μm df). The boiling range distribution led to the simulated distillation (SimDist) curve, and was obtained by using a programmable on-column (POC) injector, a wide-range FID detector and a 10 m Elite-2887 column (0.53 mm ID and 2.65 μm df). The analytical procedure used for GC analysis (BTEX and limonene, and SimDist) and GC/MS is detailed in previous works.[11,29]

3. Results and discussion

3.1. Tire pyrolysis oil

The characterization of the TPO produced by Pyrum Innovations AG is shown in Table 1. For comparison, the characterization of other TPOs used in the distillation column is also included: TPO-Greenval,[11] and TPO-ICB.[29] The former was produced in an industrial-scale pyrolysis plant in Zaragoza, Spain, capable of continuously processing approximately 5000 t per y of ELT granules. This plant is owned by Greenval Technologies and based on the single-auger technology using a license from the Spanish Council for Scientific Research (ICB-CSIC).[37] The latter came from a TRL-5 pilot-scale pyrolysis plant, which is also based on the single-auger reactor (4 kg h^{-1}) and is also located in Zaragoza. This unit is used to study different pyrolysis conditions, including not only temperature, mass flow rate and residence time, but also ELT type and size, with the goal of validating the process under industrially relevant conditions. The details of both plants are available elsewhere.[38] Although both TPO-Greenval and TPO-ICB were obtained in a similar reactor configuration and both have similar basic properties (Table 1), the presence and concentration of chemical compounds is different. As will be discussed later, this is probably due to the longer residence time of volatiles in the industrial plant compared to the pilot plant. The comparison of these TPOs with that produced by Pyrum provides an interesting backdrop to demonstrate the technical feasibility of distilling this type of alternative hydrocarbon, although they have important differences.

As it can be observed in Table 1, the results of the elemental (C, H, N and S contents) and calorific (HCV: higher calorific value) analyses are the expected ones, and also compare well with the results presented in various reviews on the subject.[12,13] It should also be noted that the basic properties of TPO-Pyrum (density, water content, flash point and pH) are consistent with those of TPO-Greenval and TPO-ICB. In general, these properties warn of the need to take precautions

 This journal is © The Royal Society of Chemistry 2025

Open Access Article. Published on 03 December 2024. Downloaded on 2/20/2026 11:20:57 AM. This article is licensed under a Creative Commons Attribution 3.0 Unported Licence.

Table 1 TPO characterization

Equipment/method	Parameter	Pyrum	Greenval	ICB
Thermo Flash 1112, UNE-EN 15307	Carbon (wt%)	88.8	88.0	89.2
	Hydrogen (wt%)	9.2	9.8	9.1
	Nitrogen (wt%)	0.9	0.9	0.6
	Sulfur (wt%)	0.8	0.7	1.1
From elemental analysis	C/H	0.80	0.75	0.82
Parr 6400, UNE-EN 15400	HCV (MJ kg^{-1})	41.6	42.0	39.2
Picnometry	Density @ 25 °C (g ml^{-1})	0.93	0.92	0.90
Crison Titromatic, ASTM E203	Water content (ppm)	165	153	148
Grabner Instruments, ASTM D6460	Flash point (°C)	<25	<25	<25
Mettler Toledo T50	pH	7.6	6.4	6.2
Simulated distillation (ASTM D2887)	IBP (°C)	64	69	90
	T_{50} (°C)	204	243	271
	FBP (°C)	532	514	534
Gas chromatography (PerkinElmer Clarus 590) – FID detector and 60 m DB-5 ms capillary column (0.25 mm ID and 0.25 μm df)	Benzene (wt%)	4.0	2.1	2.4
	Toluene (wt%)	11.4	6.2	6.2
	Ethyl-benzene (wt%)	2.6	1.0	1.3
	(*p* + *m*)-Xylene (wt%)	7.9	5.0	4.1
	o-Xylene + styrene (wt%)	2.4	1.8	2.5
	Total BTEX (wt%)	28.2	16.2	16.5
	Limonene (wt%)	0.1	2.7	5.1

during storage and use to reduce the risk of fire and corrosion. In addition, the C/H ratio (0.80) suggests a high degree of aromaticity, which is confirmed by the significant amounts of BTEX (28.2 wt%) and a practically negligible concentration of limonene. In this regard, a high concentration of BTEX is expected when both a high residence time and a high temperature profile are used during pyrolysis. It has been shown in the literature that BTEX is derived not only from the occurrence of the Diels–Alder reactions among the small chain alkenes[12,13] but also from the benzene ring in the styrene–butadiene rubber chain contained in the ELT.[39] Conversely, at very short residence times and low temperatures, the TPO typically contains large amounts of aliphatic compounds, including limonene, and the more secondary reactions occur, the lower their presence in the TPO.[40] As observed in Table 1, the TPOs previously used in the distillation column have shown lower BTEX concentrations and more limonene, consistent with the temperature and residence time used in their production.[11,29]

On the other hand, the SimDist curve of the TPO used in this work (TPO-Pyrum), as well as those discussed above (TPO-ICB and TPO-Greenval), is shown in Fig. 4. As can be seen, the boiling point distribution for all curves is very broad and appears to be in the same approximate range (64–535 °C), *i.e.* with similar initial and final boiling points (IBP and FBP, respectively). However, when comparing TPO-Pyrum to TPO-ICB and TPO-Greenval, the temperature at which 50% of the TPO evaporates (T50) is significantly lower, likely due to a higher presence of BTEX in the former. Although a possible influence on tire composition is also expected,[41] this difference is mainly related to the inherent characteristics of the pyrolysis reactor, *i.e.* the temperature profile along the reactor and the residence time of both solids and volatiles, as discussed above. The TPO studied here comes from a technology that uses higher temperatures and longer residence times, while the other TPOs were produced by using the auger

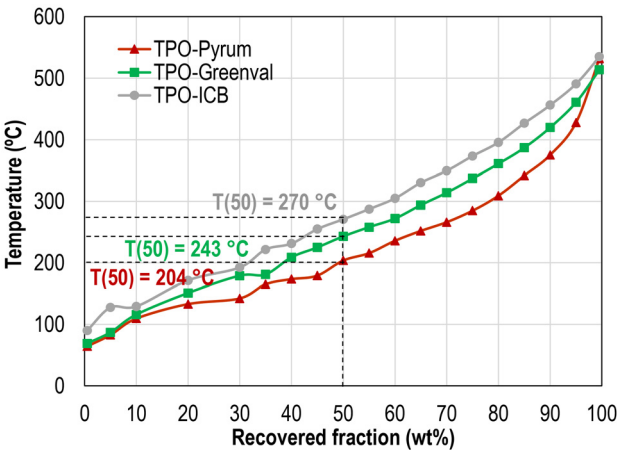

Fig. 4 Simulated distillation curve (ASTM D2887).

technology under less severe conditions. Therefore, secondary reactions are expected to dominate in the production of TPO-Pyrum, which is also reflected in the lower yield compared to the others: 40 ± 2 wt% for both TPO-Greenval and TPO-ICB.

3.2. Distillation process performance

Fig. 5 and 6 depict the pressure and temperature profiles of the distillation column, respectively, including the different stages of the process: heating (startup), TPO feed, pseudo-steady state, steady state and shutdown, for the experimental run 2. All of the experiments showed the same pattern of reaching steady state conditions, which is an important achievement in TPO refining because it reveals an appropriate control strategy that is difficult to achieve in processes involving unknown hydrocarbon feedstocks such as TPO. A detailed explanation of the distillation column in terms of pressure and

Open Access Article. Published on 03 December 2024. Downloaded on 2/20/2026 11:20:57 AM.
This article is licensed under a Creative Commons Attribution 3.0 Unported Licence.

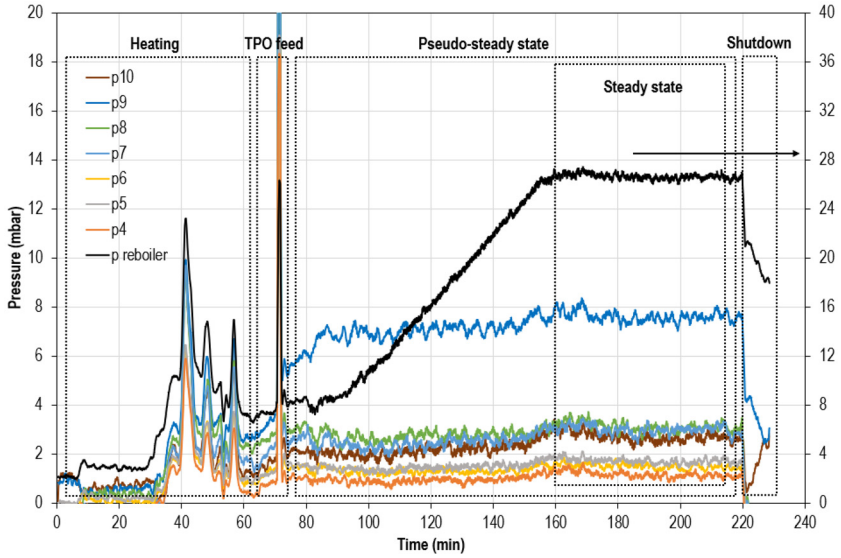

Fig. 5 Pressure profiles at 210 °C with no reflux (run 2).

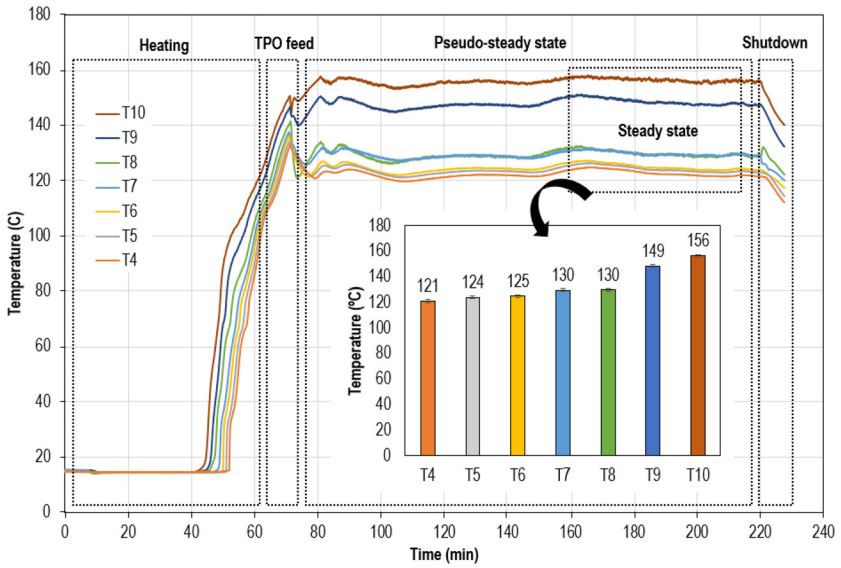

Fig. 6 Temperature profiles at 210 °C with no reflux (run # 2).

temperature patterns, including operating procedures can be found in an earlier paper.[11]

The TPO feed is characterized by a sudden increase in pressure at several points in the column, which quickly stabilizes resulting in a stable profile for both pressure and temperature. However, the pressure in the reboiler continued to increase up to 160 min of operation, which is why this stage is referred to as the pseudo-steady state. During this pseudo-steady state and later during the steady state (where the pressure in the reboiler remained unchanged), the temperatures in the column were practically the same over the operating time, and decreased from bottom to top, as expected (T10 > T4). The steady-state temperature profile of the column for all experiments is shown in the ESI (Fig. S1, S2, S3, S4, and S5†).

The heat supply at the bottom of the column and its distribution along the column appear to be adequate to promote a proper internal flow circulation of the upward vapor stream and the downward liquid stream with no visible symptoms of malfunction. Neither the temperature nor the pressure signals showed any signs of distillation problems such as flooding, suggesting stable operation conditions.[42] Except for the reboiler pressure (which always showed the highest value), all signals were quite stable. After 160 min of operation, the reboiler pressure stabilized around 26 mbar, indicating a steady state condition. Since the heavier TPO compounds are held at

 This journal is © The Royal Society of Chemistry 2025

Open Access Article. Published on 03 December 2024. Downloaded on 2/20/2026 11:20:57 AM. This article is licensed under a Creative Commons Attribution 3.0 Unported Licence.

the bottom of the column during boiling, this pressure considers not only the static head, but also some friction, expansion, contraction, and phase change phenomena. Pressure is considered as the most important parameter in distillation[43] as it controls hydraulic and thermodynamic phenomena that could lead to malfunctions.[44] Under steady state conditions, the pressure at the top of the column (commonly referred to as the column pressure) is slightly above atmospheric (2 mbar), so the pressure drop of the column is approximately 24 mbar. According to Ray and Das,[45] the pressure drop in packed distillation columns varies between 5 and 125 mm of water column per meter of packing height (in this case, between 1.5 and 43 mbar), which confirms a suitable operation and a remarkable milestone.

3.3. Yields

The LF yields for all experiments, along with the temperature at the top of the column (T4), are shown in Fig. 7. The HF yield is the remaining fraction (not shown). The relative error of these yields is less than 3% in all cases. It is also important to point out that some char particles were observed after each distillation run, mainly adhering to the resistance bars of the reboiler. Since the resulting amount was much lower than that of LF and HF, it was not considered as a product. As it can be observed in Fig. 7, the higher the temperature of the reboiler, the higher the LF yield, because the higher the fractionation severity, as expected. Light compounds tend to be enriched in the vapor stream going up the column, while the high molecular weight compounds are expected to be found in the liquid stream going down the column.

The reflux ratio also has an effect on the resulting yields, with a clear tendency for the runs performed at 230 °C, 250 °C and 270 °C. In these experiments, the LF yield decreases with the reflux ratio in comparison to the experiments without reflux. The observed lower yield of LF with reflux is consistent with the theoretical results obtained by Aspen Hysys carried out in the design of the distillation column.[29] This pattern is related to the temperature at the top of the column, which decreases when the reflux is used because some of the LF is returned to the column lowering the temperature of the rectifying section. The same finding was previously observed in the distillation column using a TPO with different properties.[11] As shown in Fig. 7, the difference between the LF yield produced with and without reflux is greater as the reboiler temperature increases because more LF is produced and therefore more liquid is introduced to the top of the column to maintain the same reflux ratio. It is worth noting again that both TPO and reflux were fed to the distillation column at room temperature, so preheating strategies for both streams may be of interest in future work to optimize the distillation operation depending on the compound or family of compounds to be recovered.

3.4. Characterization

3.4.1. BTEX in the light fraction. The concentration of BTEX compounds in the LF as a function of reboiler temperature and reflux ratio is shown in Fig. 8. The concentration of each individual compound (benzene, toluene, ethylbenzene, xylenes, and limonene) is detailed in Table S1 (ESI†). As observed in Fig. 8, the BTEX concentration reaches a maximum at 210 °C (83.2 wt%) with a very high presence of benzene and toluene (see Table S1†), and seems to be slightly favored when the reflux ratio goes to 1.5 (85.5 wt%). However, this result does not mean that all BTEX has been separated from the TPO under these experimental conditions. Residual BTEX is also found in the heavy fraction, which penalizes the BTEX recovery efficiency, as will be discussed later. To the best of the author's knowledge, this high concentration of BTEX is a remarkable milestone because: (1) no higher BTEX concentrations have been reported in the literature from the pyrolysis of ELT, either with or without the use of catalysts (see Table S3, ESI†) and (2) paving the way for scale-up of the distillation process to industrial scale to realize defossilization in the petrochemical industry. It should also be noted that BTEX production using catalysts typically compromises the TPO yield, and several factors play a key role in bringing the process to industrial scale, such as the costs associated with catalyst preparation and deactivation.

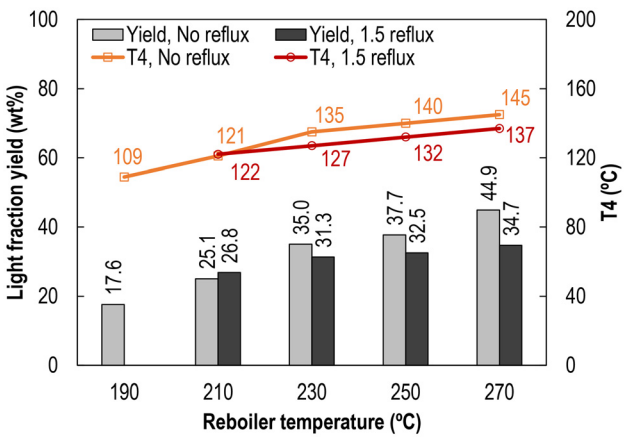

Fig. 7 Light fraction yield and T4 temperature.

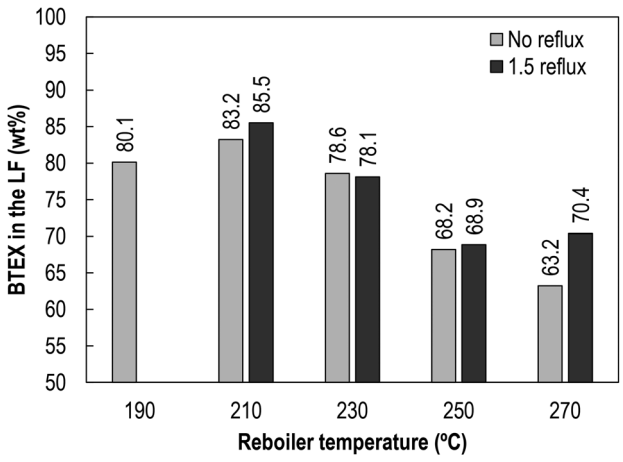

Fig. 8 BTEX concentration in the light fraction.

Open Access Article. Published on 03 December 2024. Downloaded on 2/20/2026 11:20:57 AM.
This article is licensed under a Creative Commons Attribution 3.0 Unported Licence.

Reboiler temperatures above 210 °C result in lower BTEX concentrations in the LF, probably because other compounds are also pulled out of the distillation column as the temperature at the top of the column also increases (see Fig. 7) allowing more compounds to be present in the overhead product. Fig. 8 also suggests that reflux slightly increases BTEX concentrations in the LF with a pronounced effect at the highest reboiler temperature (270 °C). Increasing the reflux ratio to 1.5 at this temperature results in a greater difference in the BTEX concentration when comparing the resulting LF obtained with and without reflux. The sharpness of the rectifying section is promoted by the reflux ratio in order to enrich the concentration of light compounds in the upward vapor stream by separating the heavier compounds contained in it. This improvement in the quality of the LF is strongly dependent on the matter and energy exchange between the liquid and vapor phases, which could be seen somehow by comparing the temperature variation along the column with and without reflux. As can be seen in Fig. S2, S3, S4 and S5 (ESI†), the reflux ratio effect results in a less flat temperature profile in the middle part of the column (the temperature difference between T8 and T4 is always lower in the experiments without reflux than in those with reflux). This pattern is expected to provide better conditions to promote the fractionation process. However, it should be noted that each stage in a packed distillation column (height equivalent to a theoretical plate) has a different efficiency along the column because the volume of the vapor stream, composition, and temperature vary with height.

3.4.2. BTEX in the heavy fraction. Fig. 9 shows the concentration of BTEX compounds in the HF as a function of reboiler temperature and reflux ratio. The concentrations of benzene, toluene, ethylbenzene and xylenes, as well as limonene are detailed in Table S2 (ESI†). Although the reflux ratio does not show a clear trend, the results for the effect of reboiler temperature are as expected: the concentration of BTEX in the HF decreases with reboiler temperature, and xylenes (which are heavier than benzene and toluene) are found to be the predominant compounds. Thus, the lowest BTEX concentration in the HF (0.9 wt%) is found at the highest reboiler temperature used in this work (270 °C), suggesting a good performance of the stripping section, as the liquid stream going down the column is enriched in heavy compounds rather than BTEX. In a feedstock destined for carbon black production, at least in the furnace process (which is the most common method of large-scale carbon black production), a low presence of BTEX in the HF is highly desirable. It is expected that the lower the BTEX in the carbon black feedstock, the lower the volatility and the higher the flash point, which is a key parameter to consider as will be discussed later. In addition, BTEX compounds do not seem to contribute properly to carbon black formation, as they affect the solid-phase nucleation mechanism and subsequent surface growth, which affects the properties of the resulting carbon black. Although there is no general consensus on the exact mechanism of carbon black formation in the furnace process, there is agreement that PAH in the carbon black feedstock are the precursors for the formation of carbon nuclei.[24]

3.4.3. C/H ratio and flash point of the heavy fraction. The C/H atomic ratio is regarded as a quick indicator to assess the aromaticity of a feedstock for carbon black production, especially for the furnace method.[46] It is expected that the higher the C/H ratio, the higher the degree of aromaticity, as is has been shown elsewhere for various carbon black feedstocks.[47–49] This tendency has been confirmed by Campuzano *et al.* in a detailed structural characterization of the different fractions obtained from the distillation of TPO.[50] Distillate TPO tends to become more aromatic as it becomes heavier, *i.e.* as the cut temperature increases, probably because the aromatic structures tend to remain in the heaviest fraction. A high C/H ratio in carbon black feedstocks typically indicates a high number of aromatic rings, which is beneficial in terms of carbon black production.[46] The complete elemental analysis of the HF is shown in Table S4 (ESI†). Based on that characterization, the C/H ratio of the resulting HF is shown in Fig. 10, including the C/H of the starting TPO for comparison (0.80).

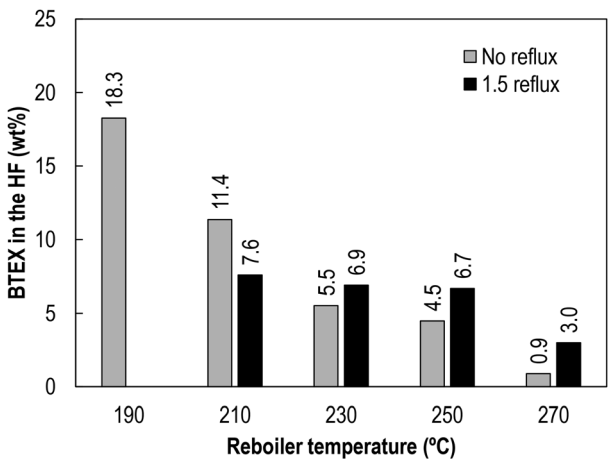

Fig. 9 BTEX concentration in the heavy fraction.

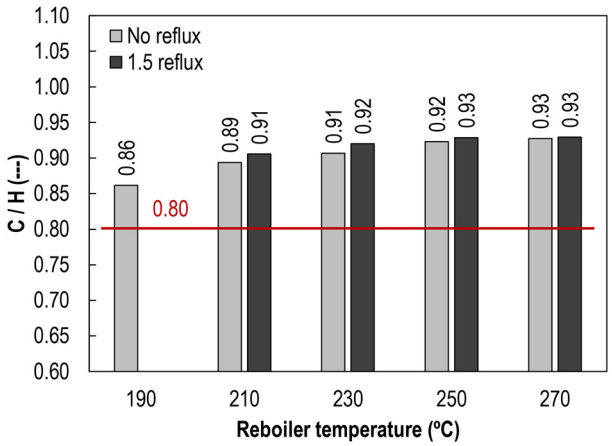

Fig. 10 C/H ratio of the heavy fraction. Red line: C/H of the starting TPO.

This journal is © The Royal Society of Chemistry 2025

Open Access Article. Published on 03 December 2024. Downloaded on 2/20/2026 11:20:57 AM.
This article is licensed under a Creative Commons Attribution 3.0 Unported Licence.

As observed, the higher the reboiler temperature, the higher the C/H ratio, suggesting a higher degree of aromaticity in the HF. The C/H ratio of the resulting HF goes from 0.86 to 0.93, and seems to be positively influenced by the reflux ratio, which indicates a notable improvement when compared to the starting TPO. The C/H ratio of typical carbon black feedstocks (including steam cracker oil, coal tar distillate, petrol vacuum residue, petrol pyrolysis tar, and petrol aromatic extract, among others) ranges from 0.594 to 1.129.[24] Using these highly aromatic feedstocks, the carbon black production is found to be between 40% and 65%.[51–53]

On the other hand, Fig. 11 shows the flash point of the HF obtained in the experimental campaign, as well as that of the starting TPO. Flash point is considered a key property in handling, transportation and storage, and for carbon black production feedstocks it is generally accepted that it should be higher than 65 °C in order to avoid potential fire hazards.[25] However, this value may vary depending on the standards of the carbon black production company. When the feedstock exceeds the regulatory flash point, flammable vapors are released, creating an explosive atmosphere if exposed to an ignition source. Typical feedstocks used to produce carbon black, such as those derived from steam crackers, catalytic crackers, and coal tar distillation, have flash points of 70 °C, 130 °C, and 90 °C, respectively.[46]

As observed in Fig. 11, the flash point of the HF increases with the reboiler temperature and is significantly improved with respect to the value of the starting TPO. This increasing trend in flash point with reboiler temperature also indicates the low presence of low molecular weight compounds in the HF. A maximum flash point of 83 °C is achieved at both 250 °C and 270 °C reboiler temperatures. The reflux ratio does not seem to help raise the flash point, but rather to lower it, at least when high reboiler temperatures are used in the distillation column. These results are quite interesting as there is no data in the literature on the variation of the flash point of the HF derived from TPO distillation.

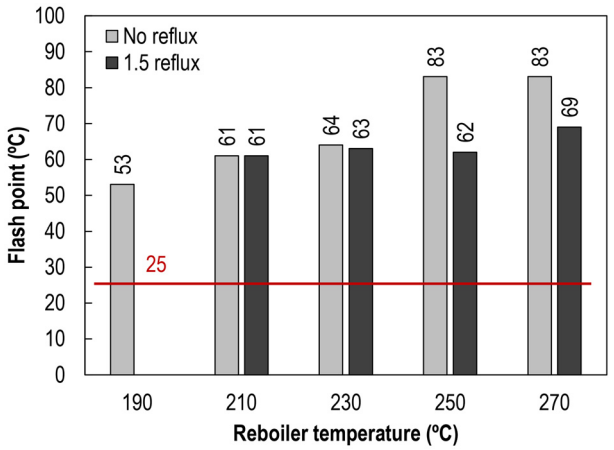

Fig. 11 Flash point of the heavy fraction. Red line: flash point of the starting TPO.

3.4.4. GC/MS results of the heavy fraction. The characterization of the resulting HF by GC/MS with respect to BTEX and PAH is shown in Fig. 12 and 13 for the experiments without and with reflux, respectively. The results for the starting TPO are also shown for comparison. These two families have been chosen to have a look at how light and heavy molecular weight compounds are concentrated in the HF. Table S5 (ESI†) shows the complete family distribution. In general, the higher the reboiler temperature, the lower the BTEX and the higher the PAH in the HF. This pattern is consistent with observations for BTEX concentration by GC, and also with that for flash point. From the GC/MS point of view, more than a half of the relative area percent of the HF obtained at 250 °C and 270 °C without reflux belongs to PAH. When the reflux ratio is increased to 1.5, the same tendency is observed for the HF produced at the highest reboiler temperature (270 °C). Furthermore, the PAH relative area percent of the resulting HF obtained with reflux ratio is always higher than that of the TPO, which supports the idea of sharpness at the rectifying section when the distillation

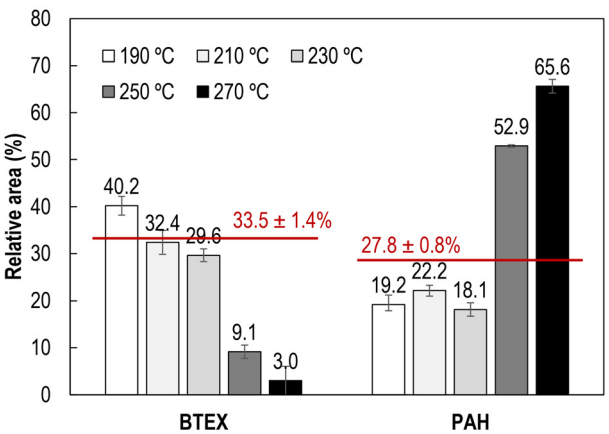

Fig. 12 GC/MS results of the heavy fraction (no reflux). Red line: values of the starting TPO.

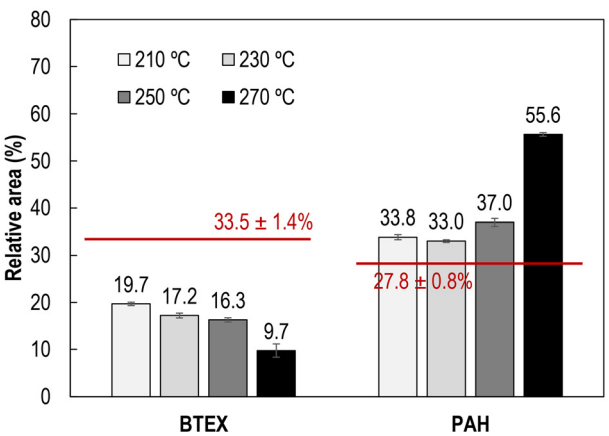

Fig. 13 GC/MS results of the heavy fraction (1.5 reflux). Red line: values of the starting TPO.

Open Access Article. Published on 03 December 2024. Downloaded on 2/20/2026 11:20:57 AM.
This article is licensed under a Creative Commons Attribution 3.0 Unported Licence.

column operates with reflux, in agreement with the observations discussed in section 3.4.1. As commented, the reflux ratio goal is to promote the separation of the most volatile compounds in the overhead product, while the stream leaving the column at the bottom is expected to have more heavier compounds.

In this work, PAH consider molecules containing only carbon and hydrogen, and their chemical structure consists of two or more fused aromatic rings fused in various arrangements with a pair of carbon atoms shared between the rings.[22] PAHs are highly desirable for carbon black production[24,49] and the more suitable feedstocks for carbon black production are mainly based on three or four ring aromatics.[46] The aromatic composition of a typical carbon black oil consists of 10–15% monocyclic, 50–60% bicyclic, 25–35% tricyclic, and 5–10% tetracyclic aromatics.[54] Therefore, the resulting HF meets the basic requirements to be considered as a feedstock for carbon black: high C/H ratio, high flash point, and high presence of PAH, which makes it possible to claim about the possibility of recovering waste-based value-added feedstocks from the distillation of TPO.

3.5. BTEX recovery efficiency and mass balance closure

The BTEX recovery efficiency in the LF was calculated based on the amount of BTEX in the LF divided by the amount contained in the TPO, and the results for all the experimental runs are shown in Fig. 14. Contrary to the trend found for the BTEX concentration in both LF and HF, the BTEX recovery efficiency increases linearly with the reboiler temperature. The highest BTEX recovery efficiency (≈100%) is found at the highest reboiler temperature tested (270 °C). However, higher BTEX recoveries do not mean higher BTEX concentration in the LF, as discussed in section 3.4.1. Interestingly, styrene has the highest boiling point of all the BTEXs (145 °C, 1 atm), which is the same temperature found at the top of the column in the experiment conducted at the highest reboiler temperature without reflux (run 5, see Fig. 6). This observation suggests that temperature control at the top of the column

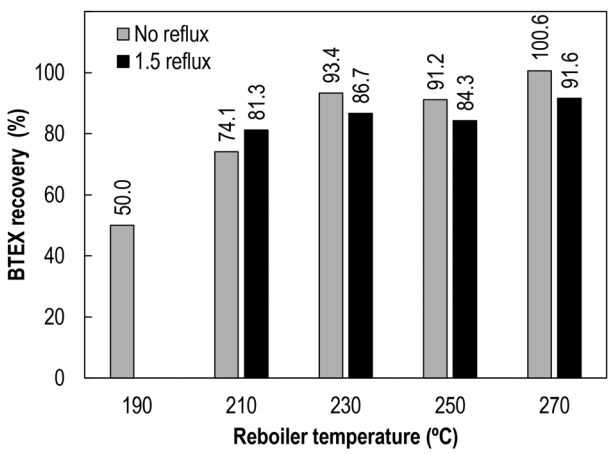

Fig. 14 BTEX recovery efficiency.

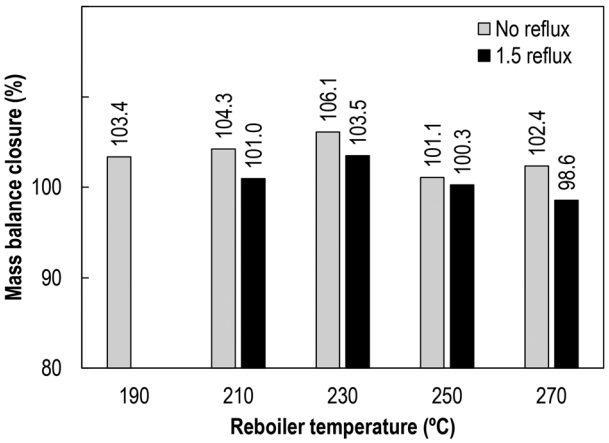

Fig. 15 Closing the BTEX mass balance.

plays a key role in achieving good fractionation of multi-component hydrocarbons such as TPO.

The mass balance closure (MBC) regarding the BTEX distribution between the inlet (TPO) and outlet streams (LF and HF) for each experiment is shown in Fig. 15. It is observed that the MBC is quite satisfactory (98.6–106.1%), taking into consideration the complexity in the operation of these plants under industrially relevant conditions, as well as the associated error not only with the measurement of the resulting yields, but also in the determination of the BTEX concentrations by GC. Therefore, the results discussed along this paper are quite reliable regarding the characteristics of the resulting products derived from the distillation of the tire pyrolysis oil, and provide an outstanding impetus for realizing defossilization in the petrochemical industry in such a way that the carbon embedded in the ELT is properly retained and converted into value-added feedstocks.

4. Conclusions

This work shows the influence of the two main control variables in packed distillation columns for the recovery of waste-based feedstocks from tire pyrolysis oil: reboiler temperature and reflux ratio. The fact that these results were obtained under industrially relevant conditions opens the door to a strong promotion of the circular economy not only in the tire sector but also in the petrochemical industry. Considering the high BTEX concentration in the TPO used for distillation, the light fraction was found to have a very high BTEX concentration with a maximum of 85.5 wt% and 81.3% recovery efficiency at 210 °C reboiler temperature and 1.5 reflux ratio. Higher severity distillation conditions result in a highly aromatic heavy hydrocarbon fraction suitable for carbon black production. For example, at 270 °C and 1.5 reflux ratio, the C/H ratio, the flash point, and the PAH presence in the resulting heavy fraction were 0.93, 69 °C and 55.6% relative area, respectively. Both the light and the heavy fractions can be

Open Access Article. Published on 03 December 2024. Downloaded on 2/20/2026 11:20:57 AM. This article is licensed under a Creative Commons Attribution 3.0 Unported Licence.

considered as value-added feedstocks for the petrochemical industry, particularly as precursor substitutes for BTEX and carbon black oil, and can meet the growing global demand for carbon-based chemicals and derivatives in a sustainable manner.

Author contributions

JD Martínez: conceptualization, data curation, formal analysis, investigation, methodology, visualization, writing – review & editing. A Sanchís, A Veses, A Kapf, JM López, MS Callén, T García: methodology, investigation, formal analysis. R Murillo: project administration, resources, supervision, writing – review & editing.

Data availability

All data supporting the findings of this study are included in the main text and the ESI.† All of relevant data are available from the corresponding authors upon reasonable request.

Conflicts of interest

There are no conflicts to declare.

Acknowledgements

This work is part of the BLACKCYCLE project (For the circular economy of tyre domain: recycling end of life tyres into secondary raw materials or tyres and other product applications) which has received funding from the European Union's Horizon 2020 research and innovation programme under grant agreement no. 869625. The authors would also like to thank the Regional Government of Aragon (DGA) for the support provided under the research groups support program and CSIC for the interdisciplinary thematic platforms SusPlast (Sustainable Plastics) and SosEcoCir (Sustainability and Circular Economy).

References

1 F. Valentini and A. Pegoretti, End-of-life options of tyres. A review, *Adv. Ind. Eng. Polym. Res.*, 2022, **5**(4), 203–213, DOI: **10.1016/j.aiepr.2022.08.006**.

2 Smithers, Global tire manufacturing output to grow 3.4% year-on-year to 2024. **https://www.smithers.com**. Access: 15/05/2023.

3 J. D. Martínez, An overview of the end-of-life tires status in some Latin American countries: proposing pyrolysis for a circular economy, *Renewable Sustainable Energy Rev.*, 2021, **144**, 111032, DOI: **10.1016/j.rser.2021.111032**.

4 Z. J. Schiffer and K. Manthiram, Electrification and decarbonization of the chemical industry, *Joule*, 2017, **1**(1), 10–14, DOI: **10.1016/j.joule.2017.07.008**.

5 J.-P. Lange, Towards circular carbo-chemicals – the metamorphosis of petrochemicals, *Energy Environ. Sci.*, 2021, **14**, 4358, DOI: **10.1039/d1ee00532d**.

6 J.-P. Lange, Managing plastic waste-sorting, recycling, disposal, and product redesign, *ACS Sustainable Chem. Eng.*, 2021, **9**, 15722–15738, DOI: **10.1021/acssuschemeng.1c05013**.

7 H. Li, H. A. Aguirre-Villegas, R. D. Allen, X. Bai, C. H. Benson, G. T. Beckham, S. L. Bradshaw, J. L. Brown, R. C. Brown, M. A. Sanchez, V. S. Cecon, J. B. Curley, G. W. Curtzwiler, S. Dong, S. Gaddameedi, J. E. Garcia, I. Hermans, M. S. Kim, J. Ma, L. O. Mark, M. Mavrikakis, O. O. Olafasakin, T. A. Osswald, K. G. Papanikolaou, H. Radhakrishnan, M. A. Sánchez Castillo, K. L. Sánchez-Rivera, K. N. Tumu, R. C. Van Lehn, K. L. Vorst, M. M. Wright, J. Wu, V. M. Zavala, P. Zhou and G. W. Huber, Expanding plastics recycling technologies: chemical aspects, technology status and challenges, *Green Chem.*, 2022, **24**, 8899–9002, DOI: **10.1039/D2GC02588D**.

8 H. Luo, H. Tyrrell, J. Bai, R. I. Muazu and X. Long, Fundamental, technical and environmental overviews of plastic chemical recycling, *Green Chem.*, 2024, **26**, 11444–11467, DOI: **10.1039/D4GC03127J**.

9 K. Ragaert, C. Ragot, K. M. Van Geem, S. Kersten, Y. Shiran and S. De Meester, Clarifying European terminology in plastics recycling, *Curr. Opin. Green Sustainable Chem.*, 2023, **44**, 100871, DOI: **10.1016/j.cogsc.2023.100871**.

10 A. J. Bowles, Á. Nievas and G. D. Fowler, Consecutive recovery of recovered carbon black and limonene from waste tyres by thermal pyrolysis in a rotary kiln, *Sustainable Chem. Pharm.*, 2023, **32**, 100972, DOI: **10.1016/j.scp.2023.100972**.

11 J. D. Martínez, A. Veses, M. S. Callén, J. M. López, T. García and R. Murillo, On fractioning the tire pyrolysis oil in a pilot-scale distillation plant under industrially relevant conditions, *Energy Fuels*, 2023, **37**(4), 2886–2896, DOI: **10.1021/acs.energyfuels.2c03850**.

12 J. D. Martínez, N. Puy, R. Murillo, T. García, M. V. Navarro and A. M. Mastral, Waste tyre pyrolysis - A review, *Renewable Sustainable Energy Rev.*, 2013, **23**, 179–213, DOI: **10.1016/j.rser.2013.02.038**.

13 P. T. Williams, Pyrolysis of waste tyres: a review, *Waste Manage.*, 2013, **33**, 1714–1728, DOI: **10.1016/j.wasman.2013.05.003**.

14 Á. Muelas, M. S. Callén, R. Murillo and J. Ballester, Production and droplet combustion characteristics of waste tire pyrolysis oil, *Fuel Process. Technol.*, 2019, **196**, 106149, DOI: **10.1016/j.fuproc.2019.106149**.

15 F. Campuzano, A. G. Abdul Jameel, W. Zhang, A.-H. Emwas, A. F. Agudelo, J. D. Martínez and S. M. Sarathy, Fuel and chemical properties of waste tire pyrolysis oil derived from a continuous twin auger reactor, *Energy Fuels*, 2020, **34**(10), 12688–12702, DOI: **10.1021/acs.energyfuels.0c02271**.

Open Access Article. Published on 03 December 2024. Downloaded on 2/20/2026 11:20:57 AM. This article is licensed under a Creative Commons Attribution 3.0 Unported Licence.

16 ASTM D8178-22, Standard Terminology Relating to Recovered Carbon Black (rCB), 2022. DOI: 10.1520/D8178-22.
17 F. Campuzano, J. D. Martínez, A. F. Agudelo Santamaría, S. M. Sarathy and W. L. Roberts, Pursuing the end-of-life tire circularity: an outlook toward the production of secondary raw materials from tire pyrolysis oil, *Energy Fuels*, 2023, **37**(13), 8836–8866, DOI: **10.1021/acs.energyfuels.3c00847**.
18 ASTM D8466-22, Standard Guide for Recovered Carbon Black—Carbon Black Test Methods for Testing rCB, 2022. DOI:10.1520/D8466-22.
19 ASTM F8474-22, Standard Test Method for Recovered Carbon Black (rCB)—Compositional Analysis by Thermogravimetry (TGA), 2022. DOI:10.1520/D8474-22.
20 G. Busca, Production of gasolines and monocyclic aromatic hydrocarbons: from fossil raw materials to green processes, *Energies*, 2021, **14**(13), 4061, DOI: **10.3390/en14134061**.
21 A. M. Niziolek, O. Onel and C. A. Floudas, Production of benzene, toluene, and xylenes from natural gas via methanol: Process synthesis and global optimization, *AIChE J.*, 2016, **62**(5), 1531–1556, DOI: **10.1002/aic.15144**.
22 G. Lezcano, I. Hita, Y. Attada, A. Bendjeriou-Sedjerari, A. H Jawad, A. Lozano-Ballesteros, M. Sun, N. Al-Mana, M. AlAmer, E.Z Albaher and P. Castaño, Selective ring-opening of polycyclic to monocyclic aromatics: A data- and technology-oriented critical review, *Prog. Energy Combust. Sci.*, 2023, **99**, 101110, DOI: **10.1016/j.pecs.2023.101110**.
23 International Energy Agency, The future of petrochemicals. Towards more sustainable plastics and fertilisers, 2018. DOI:DOI: **10.1787/9789264307414-en**. Access: 16/05/2023.
24 C. O. Okoye, I. Jones, M. Zhu, Z. Zhang and D. Zhang, Manufacturing of carbon black from spent tyre pyrolysis oil - A literature review, *J. Cleaner Prod.*, 2021, **279**, 123336, DOI: **10.1016/j.jclepro.2020.123336**.
25 H. Westenberg, H. Gromes and D. Rechenbach, Carbon black from tire-derived pyrolysis oil, *Kautsch. Gummi Kunstst.*, 2021, **6**(21), 47–51.
26 R. Palos, A. Gutiérrez, F. J. Vela, M. Olazar, J. M. Arandes and J. Bilbao, Waste refinery: the valorization of waste plastics and end-of-life tires in refinery units. A review, *Energy Fuels*, 2021, **35**(5), 3529–3557, DOI: **10.1021/acs.energyfuels.0c03918**.
27 International Energy Agency, World Energy Outlook, 2021. **https://www.iea.org/reports/world-energy-outlook-2021**, Access: 16/05/2023.
28 International Energy Agency, Key World Energy Statistics, 2021. **https://www.iea.org/reports/key-world-energy-statistics-2021**, Access: 16/05/2023.
29 J. D. Martínez, A. Sanchís, A. Veses, M. S. Callén, J. M. López, T. García and R. Murillo, Design and operation of a packed pilot scale distillation column for tire pyrolysis oil: Towards the recovery of value-added raw materials, *Fuel*, 2024, **358**, 130266, DOI: **10.1016/j.fuel.2023.130266**.
30 G. García-García, M. A. Martín-Lara, M. Calero and G. Blázquez, Environmental impact of different scenarios for the pyrolysis of contaminated mixed plastic waste, *Green Chem.*, 2024, **26**, 3853–3862, DOI: **10.1039/D3GC04396G**.
31 P. T. Anastas and J. C. Warner, *Green chemistry: theory and practice*, *Oxford University Press*, 2000.
32 R. A. Sheldon, The E factor at 30: a passion for pollution prevention, *Green Chem.*, 2023, **25**, 1704–1728, DOI: **10.1039/D2GC04747KB**.
33 Pyrolysis method and apparatus for carrying out the method, *International Patent*, WO 2010/127664A1, Inventor: Klaus-Peter Schulz, Assignee: Pyrum Innovations International S.A.
34 Thermal reactor, *International Patent*, WO 2012/092924A1, Inventor: Klaus-Peter Schulz, Assignee: Pyrum Innovations International S.A.
35 W. L. McCabe, J. C. Smith and P. Harriot, Distillation, in *Unit Operations of Chemical Engineering*, McGraw-Hill Inc., 7th edn, 2004, ch. 21.
36 J. M. Coulson and J. F. Richardson, Distillation, in *Chemical Engineering Design*, Butterworth-Heinemann, 2005, ch. 11.
37 Procedimiento y aparato de termolisis de polimeros de desecho, *International Patent*, WO 2012/127085A1, Inventor: Ramón Murillo Villuendas, Assignee: Consejo Superior de Investigaciones Científicas, Tecnologias Ineditas Medioambientales S L.
38 A. Veses, J. D. Martínez, A. Sanchís, J. M. López, T. García, G. García and R. Murillo, Pyrolysis of end-of-life tires: moving from a pilot prototype to a semi-industrial plant using auger technology, *Energy Fuels*, 2024, **38**(17), 17087–17099, DOI: **10.1021/acs.energyfuels.4c02748**.
39 J. Li, D. Zheng, Z. Yao, S. Wang, R. Xu, S. Deng, B. Chen and J. Wang, Formation mechanism of monocyclic aromatic hydrocarbons during pyrolysis of styrene butadiene rubber in waste passenger car tires, *ACS Omega*, 2022, **7**(47), 42890–42900, DOI: **10.1021/acsomega.2c04994**.
40 N. M. Mkhize, P. van der Gryp, B. Danon and J. F. Görgens, Effect of temperature and heating rate on limonene production from waste tyre pyrolysis, *J. Anal. Appl. Pyrolysis*, 2016, **120**, 314–320, DOI: **10.1016/j.jaap.2016.04.019**.
41 A. Sanchís, A. Veses, J. D. Martínez, J. M. López, T. García and R. Murillo, The role of temperature profile during the pyrolysis of end-of-life-tyres in an industrially relevant conditions auger plant, *J. Environ. Manage.*, 2022, **317**, 115323, DOI: **10.1016/j.jenvman.2022.115323**.
42 H. Z. Kister, Common Techniques for Distillation Troubleshooting, in *Distillation Operation and Applications*, ed. A. Górak and H. Schoenmakers, Elsevier Inc., 2014, ch. 2.
43 H. Z. Kister, *Distillation Operation*, McGraw Hill, 1990.
44 Z. Li, Y. Chen, Y. Yang, C. Liu, M. Lucquiaud and J. Jia, Flow regime transition in countercurrent packed column monitored by ECT, *Chem. Eng. J.*, 2021, **420**(Part 1), 129841, DOI: **10.1016/j.cej.2021.129841**.

 This journal is © The Royal Society of Chemistry 2025

Open Access Article. Published on 03 December 2024. Downloaded on 2/20/2026 11:20:57 AM.
This article is licensed under a Creative Commons Attribution 3.0 Unported Licence.

45 S. Ray and G. Das, Distillation, in *Process Equipment and Plant Design. Principles and Practices*, ed. S. Ray and G. Das, Elsevier Inc., 2020, ch. 11.
46 J. B. Donnet, R. C. Bansal and M. J. Wang. Carbon Black, *Science and technology*, CRC Press, 2nd edn, 1993.
47 M. Srivastava, I. D. Singh and H. Singh, Structural characterization of petroleum based feedstocks for carbon black production, *Pet. Sci. Technol.*, 1999, **17**(1–2), 67–80, DOI: **10.1080/10916469908949707**.
48 S. V. Shurupov, Some factors that govern particle carbon formation during pyrolysis of hydrocarbons, *Proc. Combust. Inst.*, 2000, **28**(2), 2507–2514, DOI: **10.1016/S0082-0784(00)80666-9**.
49 A. Javadi, S. Soltanieh, S. Sahebdelfar, D. Bastani and K. Javadi, Estimation of temperature and residence time of carbon black oil furnace industrial reactors, *Proceedings of IMECE2006*, IMECE2006-15671, 2006, pp. 69–77. DOI: **10.1115/IMECE2006-15671**.
50 F. Campuzano, A. G. Abdul Jameel, W. Zhang, A.-H. Emwas, A. F. Agudelo, J. D. Martínez and S. M. Sarathy, On the distillation of waste tire pyrolysis oil: A structural characterization of the derived fractions, *Fuel*, 2021, **290**, 120041, DOI: **10.1016/j.fuel.2020.120041**.
51 M.-J. Wang, C. A. Gray, S. A. Reznek, K. Mahmud and Y. Kutsovsky, *Kirk-Othmer Encyclopedia of chemical technology: Carbon black*, 2003. DOI: **10.1002/0471238961.0301180204011414.a01.pub2**.
52 A. Boulamanti and J. A. Moya. Energy efficiency and GHG emissions: Prospective scenarios for the chemical and petrochemical Industry, Science for policy report: EUR 28471 EN, 2017. DOI:DOI: **10.2760/20486**.
53 Y. Abdallas Chikri and W. Wetzels, *Decarbonization options for the Dutch carbon black industry*. PBL Netherlands Environmental Assessment Agency, TNO, 2020. **https://resolver.tno.nl/uuid:38ed9922-ce9c-4e8c-8388-e13276694a08m**.
54 European Commission, Integrated pollution prevention and control. Reference document on best available techniques for the manufacture of large volume inorganic chemicals - solids and others industry, 2007. **https://eippcb.jrc.ec.europa.eu/reference/large-volume-inorganic-chemicals-solids-and-others-industry**.